DISPERSION OF ELECTROMAGNETIC DAMPING

by

N. Matsumoto, J. P. Verboncoeur, and K. L. Cartwright

Memorandum No. UCB/ERL M96/88

20 December 1996

DISPERSION OF ELECTROMAGNETIC DAMPING

by

N. Matsumoto, J. P. Verboncoeur, and K. L. Cartwright

Memorandum No. UCB/ERL M96/88

20 December 1996

ELECTRONICS RESEARCH LABORATORY

College of Engineering
University of California, Berkeley
94720

Dispersion of electromagnetic damping

N.Matsumoto*, J.P.Verboncoeur and K.L.Cartwright

Electronics Research Laboratory
University of California
Berkeley, CA 94720-1774, USA

Abstract

A temporal filtering scheme has been implemented in OOPIC for the purpose of damping high frequency noise thus reducing numerical heating. This noise is generated from the smaller number of computer particles compared with the number of realistic charged particles in plasma. To understand the damping, the dispersion relation is plotted with respect to various damping parameters and Courant condition. Then the effect of noise damping and the loss of energy, respectively, are examined.

As a result, it is found that some spatial profiles have been smoothed in place of some energy loss. That is, there is a trade off between dispersion and dissipation.

*Advanced Technology Research Laboratories,
Sumitomo Metal Industries Ltd.
1-8, Fuso-cho, Amagasaki, Hyogo 660, Japan

Naoki Matsumoto was a visitor with our Plasma Theory and Simulation Group here in Berkeley from January through July, 1996. He was here to learn and to apply our 2d3v EM code OOPIC to the Surface Wave Plasma reactor now operating at Sumitomo Metals Industries, in Amagasaki, Japan. We found this simulation to be very challenging. His physics results are presented in another report. This report covers a change in the numerical methods used in OOPIC.

Prof. C. K. Birdsall July 1996

1 Introduction

A noise damping scheme reducing numerical heating is advantageous in electromagnetic Particle In Cell (PIC) code for the simulation of realistic plasma source. Noise is generated by numerous mechanism, such as when particles cross cell boundaries. This is enhanceded when there are few computer particles per Debye sphere. Long simulation running in such a case sometimes causes unphysical energy gain with an increase in electron and ion temperatures, leading to a physically inaccurate model. Increasing the number of computer particles can increase accuracy, but is not practical because too much CPU time and memory are needed. Several approaches to reduce this unphysical noise have been proposed by A. Friedman et al [1], [2]. Here the temporal filtering scheme, one of such approaches, will be presented for the cure of the noise problem.

2 Model

One of features of this temporal filtering scheme is that the damping parameter is continuously tunable from the C_0 scheme which uses one past data point to the D_1 scheme which uses all past values recursively. The C_0 scheme and the D_1 scheme represent the ordinary leapfrog method (no damping) and the explicit method (full damping), respectively.

Because the scheme is independent of geometries and boundary conditions, it is easy to implement.

For Maxwell's equation, we define the lag-averaged electric field like this:

$$\bar{\mathbf{E}}^{n-1} = (1-\frac{\theta}{2})\mathbf{E}^{n} + \frac{\theta}{2}\bar{\mathbf{E}}^{n-2}, 0 \le \theta \le 1. \tag{1}$$

The new electric and magnetic fields are then,

$$\mathbf{E}^{n+1} = \mathbf{E}^{n} + c\Delta t \nabla \times \mathbf{B}^{n+\frac{1}{2}} - 4\pi \mathbf{J}^{n+\frac{1}{2}}\Delta t, \tag{2}$$

$$\mathbf{B}^{n+\frac{3}{2}} = \mathbf{B}^{n+\frac{1}{2}} - c\Delta t \nabla \times [(1+\frac{\theta}{4})\mathbf{E}^{n+1} - \frac{1}{2}\mathbf{E}^{n} + (\frac{1}{2}-\frac{\theta}{4})\bar{\mathbf{E}}^{n-1}]. \tag{3}$$

The one dimensional dispersion relation for this scheme is

$$\sin^2(\frac{\omega\Delta t}{2}) = \nu^2\sin^2(\frac{k\Delta x}{2})[1 - \frac{2\theta\sin^2(\frac{\omega\Delta t}{2})}{2e^{-i\omega\Delta t} - \theta}] \tag{4}$$

where ν is a Courant number, $c\Delta t/\Delta x$, θ is the damping parameter, varied from 0 to 1. In particular, for small $\omega\Delta t$, we can distinguish between the real part and the imaginary part. The imaginary part is called the damping rate.

The real and imaginary part can be approximated for small values $\omega\Delta t$ as follows.

$$\omega_r\Delta t = 2\Omega[1 + \Omega^2(\frac{1}{6} - \frac{\theta}{2-\theta}) + \cdots] \tag{5}$$

$$\gamma\Delta t = -\frac{8\theta}{(2-\theta)^2}\Omega^4 + \cdots \tag{6}$$

where, we define the parameter

$$\Omega \equiv \nu\sin(\frac{k\Delta x}{2}) \tag{7}$$

For the two dimensional dispersion relation with $\Delta x = \Delta y$, we need only change the Courant number ν to $\sqrt{2}\nu$.

3 Results

Here, some dispersion relations with damping rates are shown in one dimension with respect to damping parameter, as well as Courant numbers, for electromagnetic waves.

Fig.1 shows an ordinary dispersion relation. The branch of ν=1.2 indicates an error because the phase velocity exceeds the light velocity. No dispersion error occurs for ν=1.0, which is marginally stable.

Fig.2 and Fig.3 show dispersion relations with damping rates for the case θ=0.5 and 1, respectively. For θ=0.5, greater than ν=0.6 produces $v_{phase}>c$ at $k\Delta x \geq 2$. Accordingly, these large ν's are not recommended for simulation. For θ=1, all damping rates are much larger than for θ=0.5 as Courant number is increased with ν>0.6 not recommended. We have to pay attention to the damping rate when it has negative value.

Next, the dependence of the damping parameter θ is shown in Fig.4 thru Fig.7 for the case ν=0.5, which is a value used in a typical simulation. We can see that the large θ implies larger damping rate and the slower phase velocity of the electromagnetic wave. Also, the locus of numerical solutions, obtained by replacing $\omega=\omega_r+\gamma$ by $Z=\exp(-\omega\Delta t)$, is also plotted on the complex plane in Fig.8 for the same Courant number. All roots start with Re[Z]=1, arc to the left as kdx is increased. Then the root of θ=1 moves toward the origin while the root of θ=0 still follows the unit circumference. That is, moving toward the origin means the mode is damped.

Next, the effect of the noise damping was examined to observe the characteristics of the temporal filtering scheme. For this purpose, we implemented the temporal filtering scheme in OOPIC to simulate a Surface Wave Plasma (SWP) discharge, whose configuration is shown schematically in Fig.9. No power was inputed to make a distinction between physical and unphysical heating. The simulation ran 9000 timesteps.

Some results are shown in Fig.10 and 11 when compared with θ= 0, 1.0 In ordinary simulation, magnetic fields cause the energy to increase in time in spite of lack of input power, the particles interact with electric fields, eventually making the number of particles increase. This is of course unphysical heating.

On the other hand, the simulation inplemented the temporal filtering scheme shows the stable energy transition as a result of removing unphysical high frequency noise. As seen in Fig.12 and 13, the temporal filtering scheme makes E_y smoother. But this smoothness means some electromagnetic energy loss simultaneously.

Therefore, it was examined for various θ how much energy was lost by using the temporal filtering scheme when an TEM wave pulse was set to propagate in one direction. The wave pulse was 1.2×10^{-10}sec in width and 10^4V/m in amplitude, and the Courant number was 0.5. The square of normalized Bz was observed. The damping rate was also calculated for both theoretical and simulation results as in Fig.14. The loss of energy increased with θ and was 40% for θ=1 after 400 steps.

We can see from above discussions that there is a balance needed between heating and smoothing for the optimum simulation.

4 Conclusion

Temporal filtering scheme which has been added to OOPIC was investigated for the purpose of damping noise which causes numerical heating.

The dispersion relation was presented with respect to various damping parameters as well as Courant conditions for electromagnetic wave.

The effect of noise damping and the loss of energy, respectively, are also examined.

It is found that profiles are smoothed and energy is lost. That is, there is a trade off between dispersion and dissipation.

5 Acknowledgments

The author greatly appreciates useful discussions with Dr. V. P. Gopinath, D. Cooperberg and Prof. C. K. Birdsall at EECS Dept in University of California, Berkeley.

The author would also like to thank Y. Morioka, T. Akahori, Dr. K . Komachi, T. Ebata, Dr. Hinotani, Dr. Sato and Dr. S. Kobayashi of Sumitomo Metal Industries, Amagasaki, Japan, for supporting his visit to Berkeley, January - July 1996.

6 Reference

References

[1] A.Friedman, "Damped Time Advance Methods for Particles and EM Fields" US-Japan Workshop on Advanced Computer SImlation Techniques Applied to Plasma and Fusion (1990)

[2] P.Rambo, J.Ambrosiano, A.Friedman and D.E.Nielsen, "Temporal and Spatial Filtering Remedies for Dispersion in Electromagnetic Particle Codes" American. Phys. Soc. (1989)

[3] C.K. Birdsall and A.B. Langdon, "Plasma Physics Via Computer Simulation" (Adam Hilger, Bristol, 1991).

[4] J.P.Verboncoeur, A.B.Langdon and N.T.Gladd, "An object-oriented electromagnetic PIC code", Comp. Phys. Comm. 87, 199 (1995).

[5] M.A.Lieberman and A.J.Lichtenberg, "Principle of Plasma Discharge and Materials Processing" (Wiley Interscience, NY, 1994).

7 Figure Captions

Fig.1 The ordinary leap-frog dispersion relation.

Fig.2 The dispersion relation with TFS for θ=0.5.

Fig.3 The dispersion relation with TFS for θ=1.0.

Fig.4 The dispersion relation at large kΔx for ν=0.5.

Fig.5 The damping rate at large kΔx for ν=0.5.

Fig.6 The dispersion relation at small kΔx for ν=0.5.

Fig.7 The damping rate at small kΔx for ν=0.5.

Fig.8 The locus of numerical solutions of Z=exp(-$\omega\Delta$t) for ν=0.5.

Fig.9 The schematic configuration of the Surface Wave Plasma (SWP) model.

Fig.10 The time evolution of field and kinetic energies without TFS.

Fig.11 The time evolution of field and kinetic energies with TFS.

Fig.12 The spatial profile of E_y without TFS.

Fig.13 The spatial profile of E_y with TFS.

Fig.14 The energy loss of an TEM wave pulse and the damping rate.

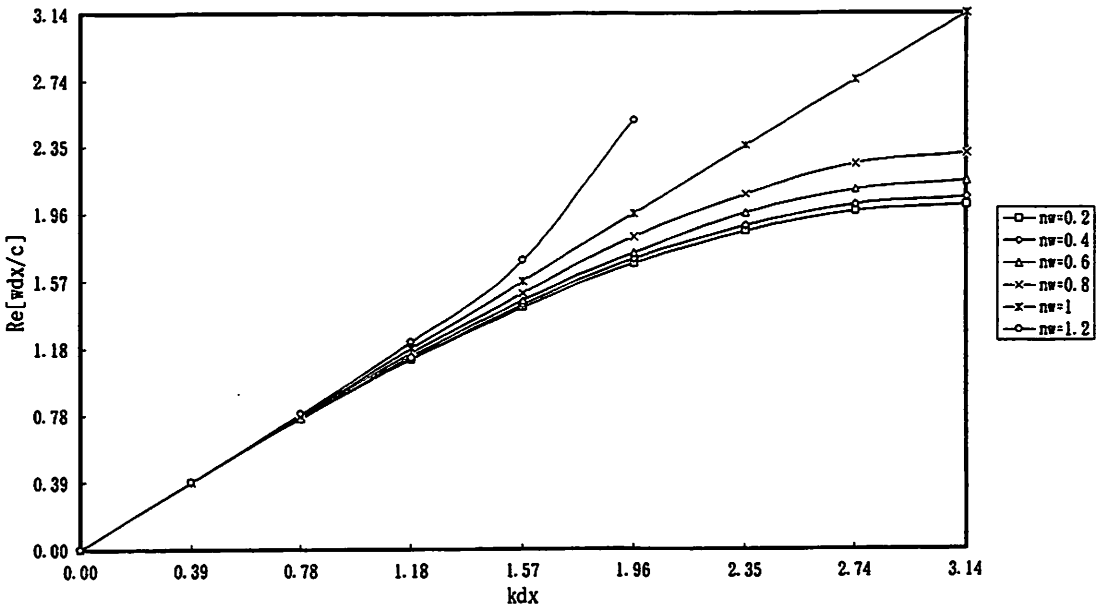

Fig.1 The ordinary leap-frog dispersion relation.

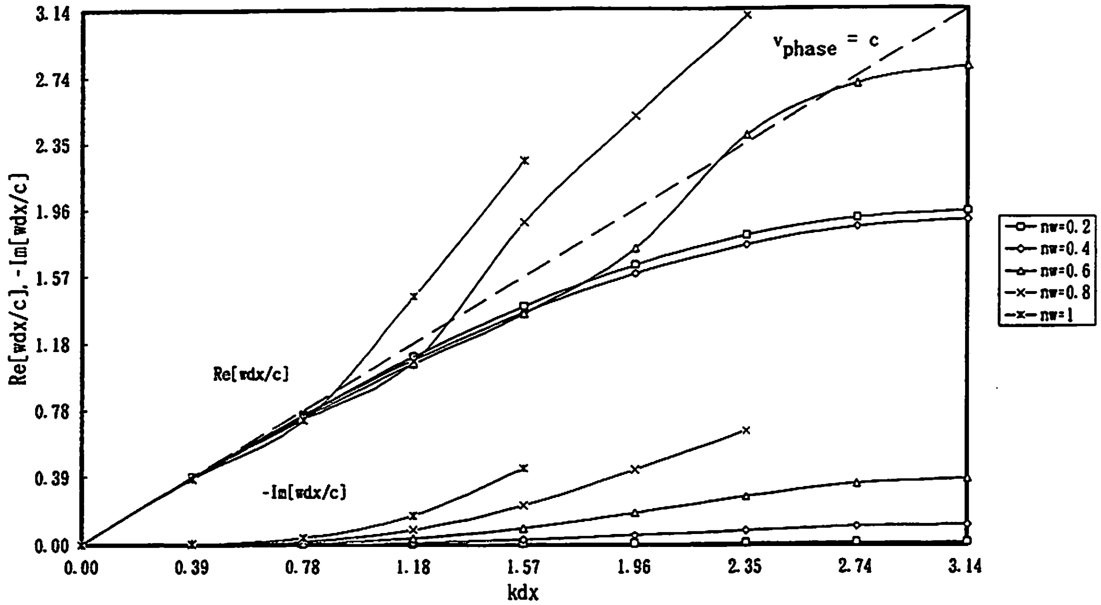

Fig.2 The dispersion relation with TFS for θ=0.5.

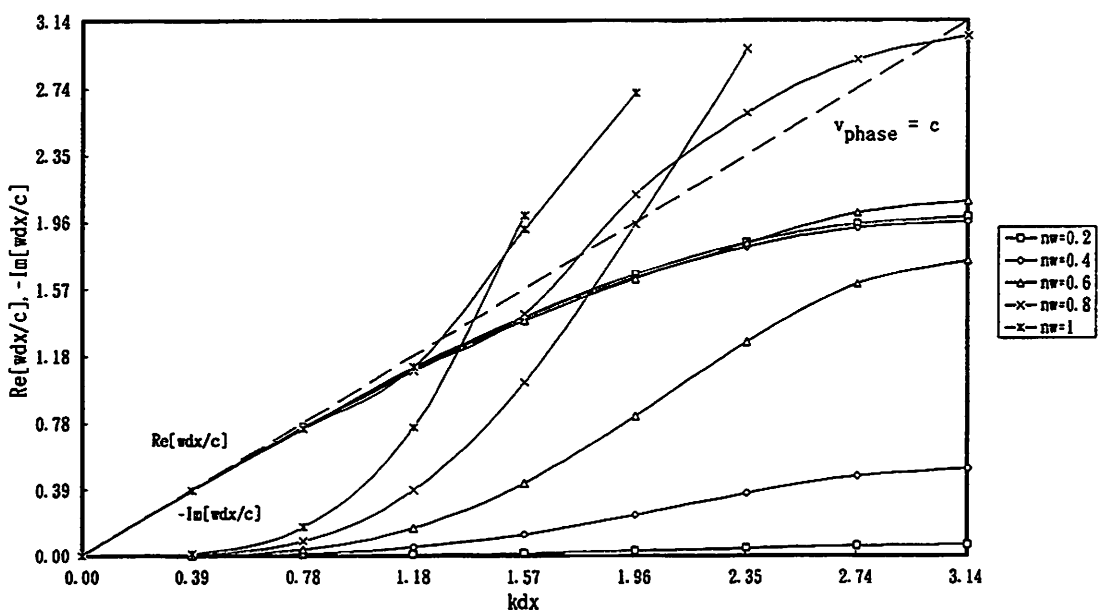

Fig.3 The dispersion relation with TFS for θ=1.0.

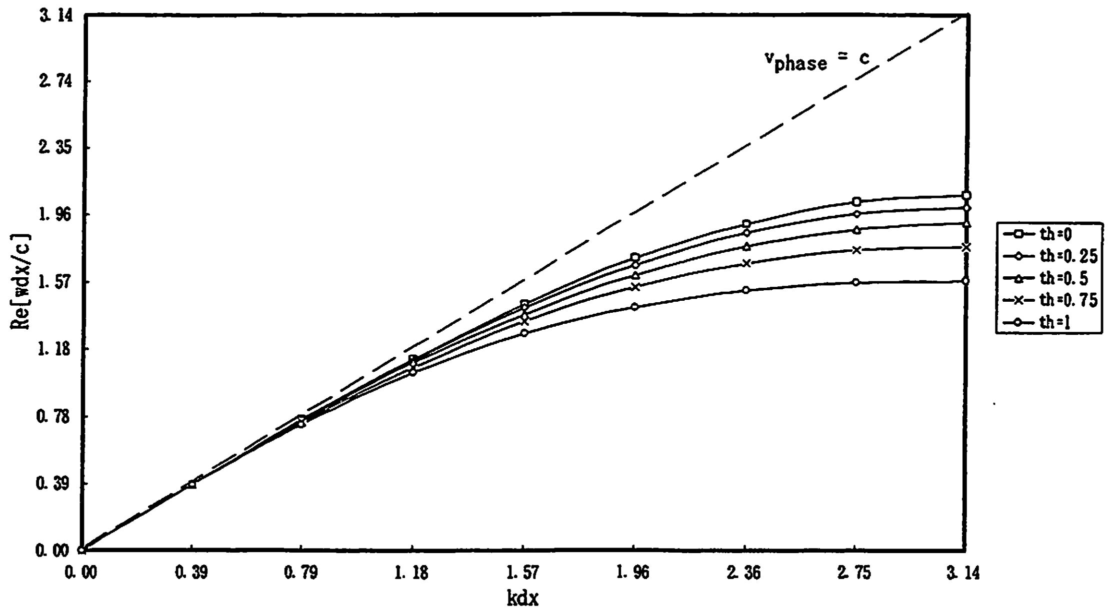

Fig.4 The dispersion relation at large kΔx for ν=0.5.

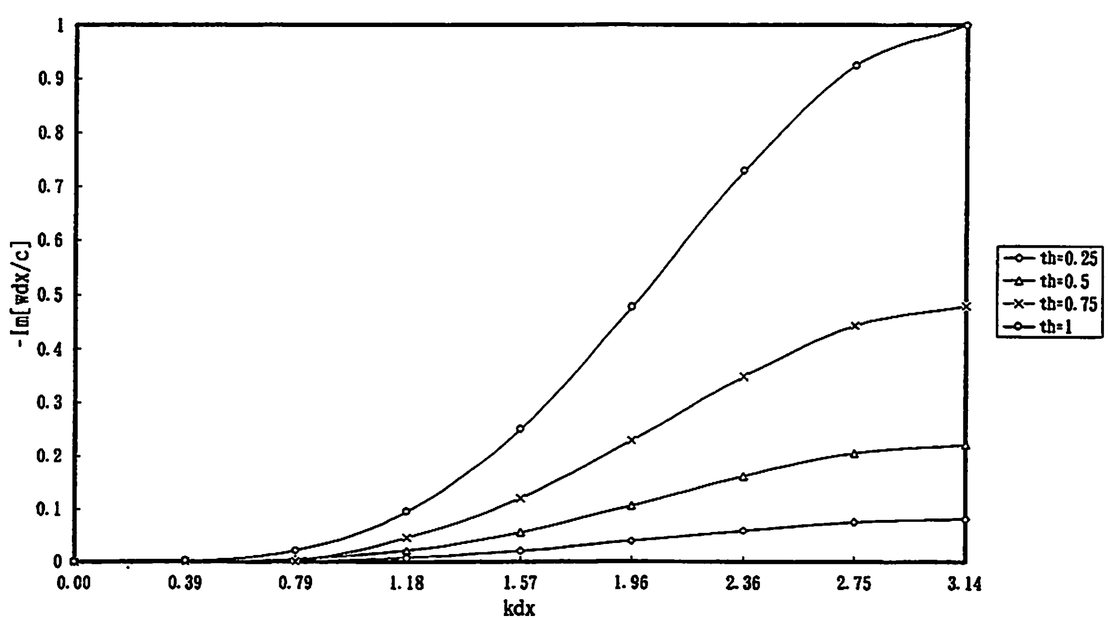

Fig.5 The damping rate at large kΔx for ν=0.5.

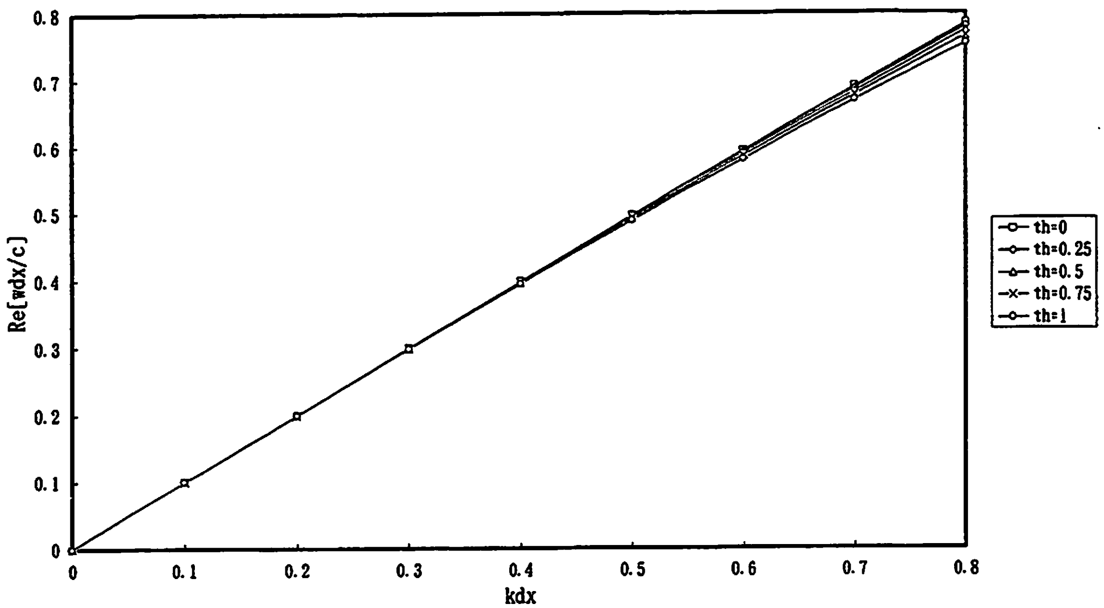

Fig.6 The dispersion relation at small $k\Delta x$ for ν=0.5.

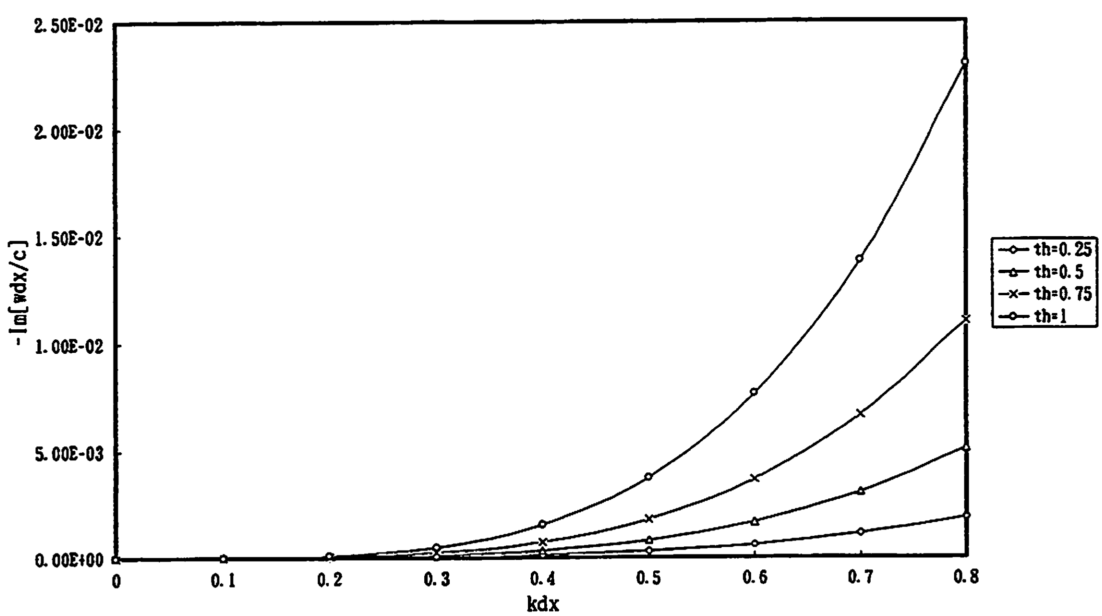

Fig.7 The damping rate at small $k\Delta x$ for ν=0.5.

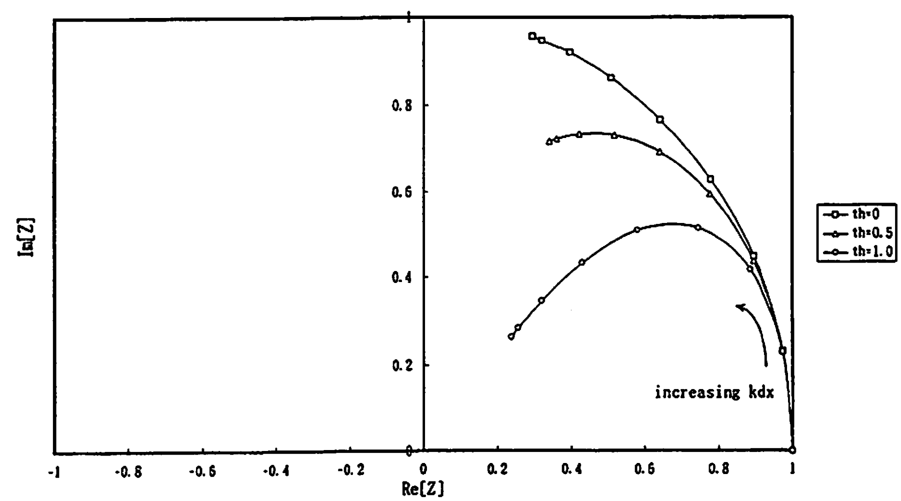

Figure 8: The locus of numerical solutions of Z=exp(-$\omega\Delta$t) for ν=0.5.

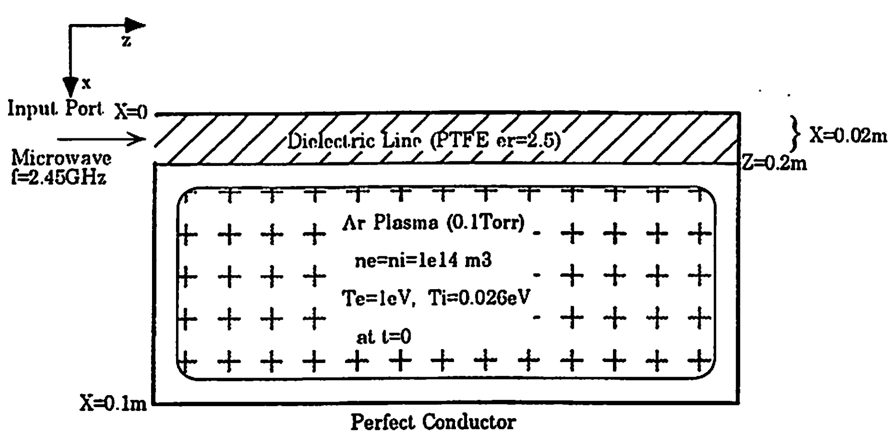

Figure 9: The schematic configuration of the Surface Wave Plasma (SWP) model.

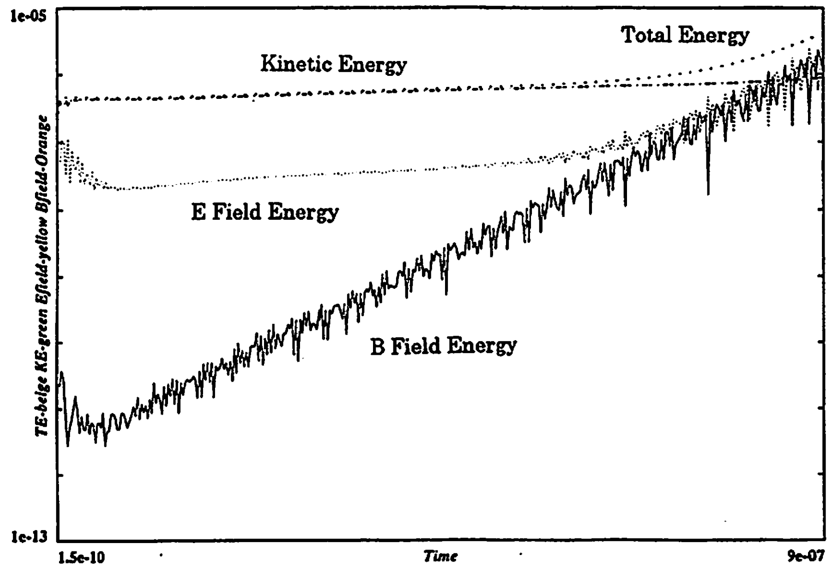

Figure 10: The time evolution of magnetic fields without TFS.

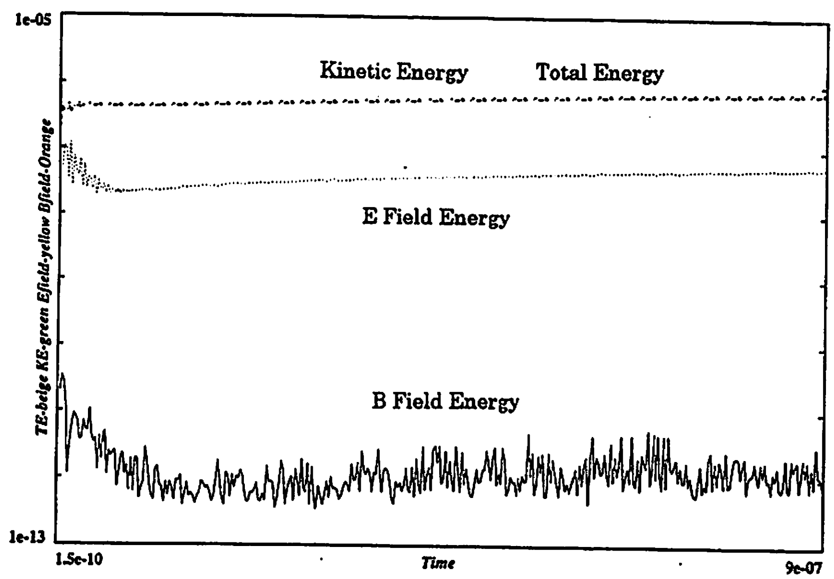

Figure 11: The time evolution of magnetic fields with TFS.

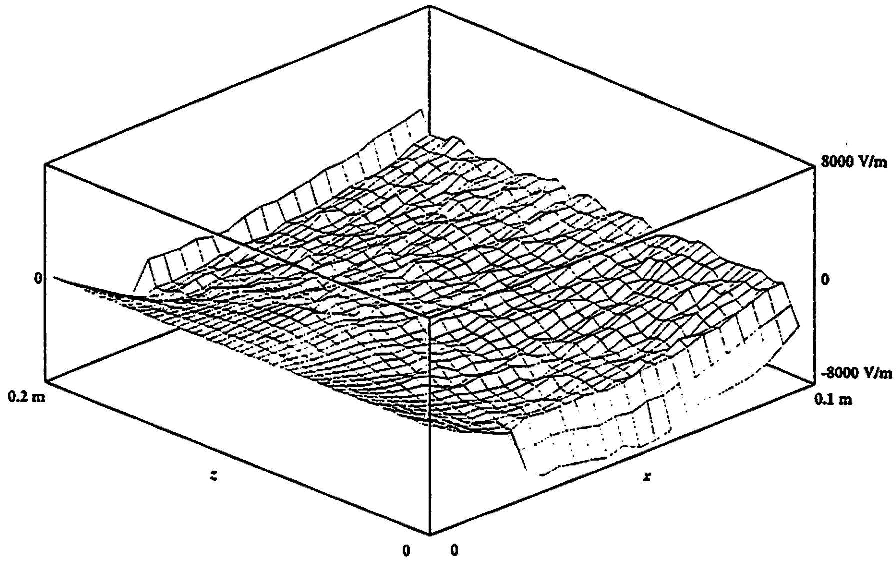

Figure 12: The spatial profile of E_y without TFS.

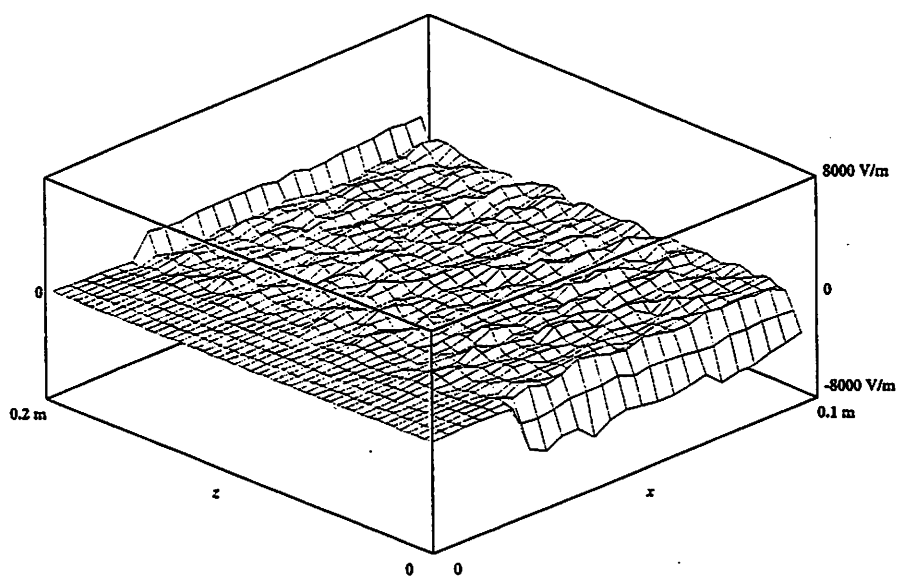

Figure 13: The spatial profile of E_y with TFS.

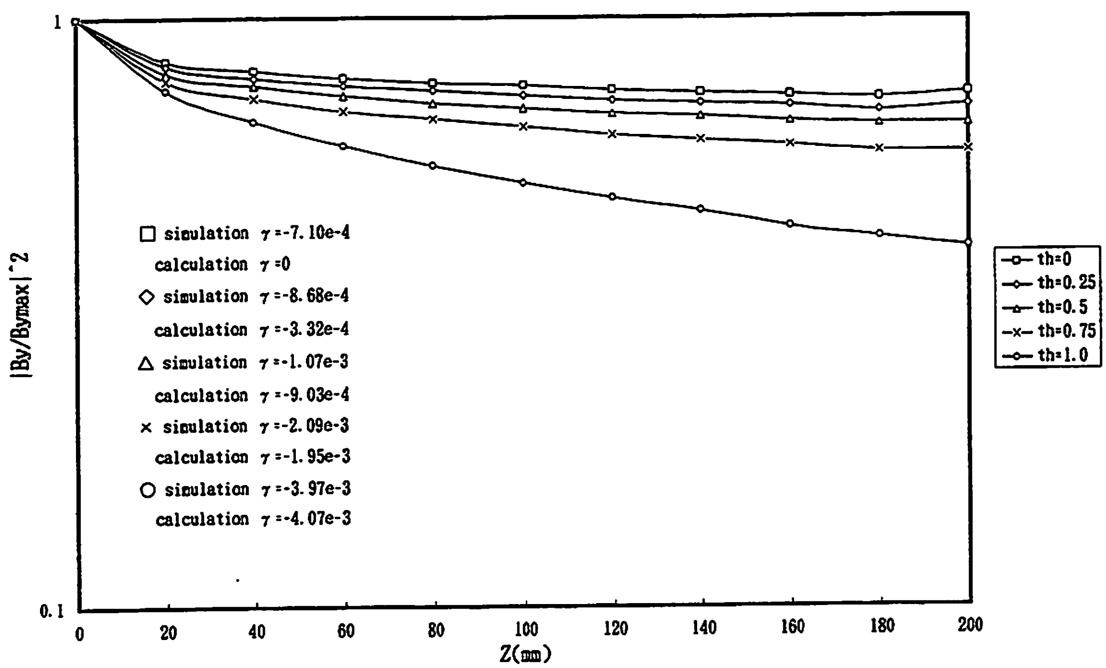

Fig.14 The energy loss of an TEM wave pulse and the damping rate.